JACS
JOURNAL OF THE AMERICAN CHEMICAL SOCIETY
Article
pubs.acs.org/JACS

Explaining the Highly Enantiomeric Photocyclodimerization of 2-Anthracenecarboxylate Bound to Human Serum Albumin Using Time-Resolved Anisotropy Studies

Denis Fuentealba,[†,∥] Hanako Kato,[‡] Masaki Nishijima,[§] Gaku Fukuhara,[‡] Tadashi Mori,[‡] Yoshihisa Inoue,*[,‡] and Cornelia Bohne*[,†]

[†]Department of Chemistry, University of Victoria, P.O. Box 3065, Victoria, British Columbia, Canada V8W 3 V6

[‡]Department of Applied Chemistry and [§]Office for University−Industry Collaboration, Osaka University, 2-1 Yamada-oka, Suita 565-0871, Japan

Supporting Information

ABSTRACT: The mechanism for the high enantiomeric excess (ee) (80−90%) observed in the photocyclodimerization of 2-anthracenecarboxylate (AC) in the chiral binding sites of human serum albumin (HSA) was studied using fluorescence anisotropy. A long rotational correlation time of 36 ns was observed for the excited states of the ACs bound to the HSA site responsible for the high ee, suggesting that the ACs have restricted rotational mobility in this site. The ACs in this site have the same prochiral face protected by the protein, and this protection is responsible for the high ee observed. These insights provide a strategy for the rational design of supramolecular photochirogenic systems.

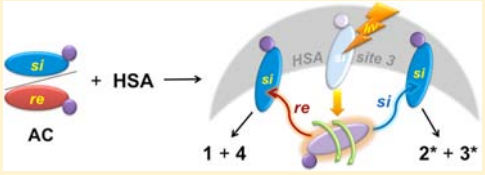

INTRODUCTION

Chirality is ubiquitous in nature, and controlling molecular chirality is essential in many areas of chemistry and biology. The supramolecular approach to catalytic[1] and photochemical asymmetric syntheses[2,3] has the advantage that chirality is imposed through noncovalent interactions, and the system's reversibility provides opportunities for product turnover.[1,4,5] From a different perspective, photochemistry enables selectivity by judicious excitation of reactants.[6] The combination of these two approaches is very effective and has been explored for a variety of host systems.[2,3]

The interactions of the ground and excited states of the guest with the chiral host affect the degree of photochirogenesis observed. Potentially, the stereoselectivity achieved through ground-state complexation can be enhanced for the excited-state reaction, because the interactions of these two states with the host may be different. It is likely that excited-state dynamics does not greatly affect the stereoselectivity of tightly packed or stacked supramolecular systems, such as for reactions in some systems involving cyclodextrins[6−9] and for hydrogen-bonding templates,[4,10−12] because no mobility can occur before the excited guests undergo reaction. For bimolecular reactions that are dynamic, that is, do not occur immediately for reactants that are in close proximity, the mobility of the excited guest inside the chiral host or between the inside and outside of the host may affect the outcome of the stereoselectivity. The influence of the excited-state dynamics, which may amplify the stereoselectivity, is unique to the supramolecular photochemical approach, since for thermal reactions, only the selectivity of the ground state is relevant. However, the influence of the excited-state dynamics has only been inferred[3] but has not been directly probed. Elucidation of the importance of the roles of excited-state dynamics or the internal mobility of reactants inside hosts will provide essential information on controlling the stereochemical outcome of supramolecular chirogenesis. In the present work, we used fluorescence anisotropy measurements to study the mobility of an excited reactant inside the host. The bimolecular photocyclodimerization of 2-anthracenecarboxylate (AC, Scheme 1) was chosen as the model reaction because this reaction has been studied in various supramolecular systems, such as cyclodextrins, hydrogen-bonding templates, and serum albumins.[3] Human serum albumin (HSA) was chosen as the host, since it afforded the

Scheme 1. Photocyclodimerization of 2-Antracenecarboxylate (AC)[a]

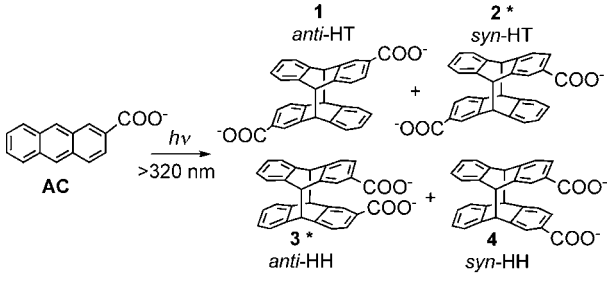

[a]The absolute configurations of **2*** and **3*** are arbitrary, and HT and HH stand for head-to-tail and head-to-head dimers, respectively.

Received: August 16, 2012
Published: December 13, 2012

   dx.doi.org/10.1021/ja3081555 | J. Am. Chem. Soc. 2013, 135, 203−209

highest enantiomeric excess (ee) to date (80−90%) for the AC photocyclodimerization in a supramolecular system.[13,14]

Proteins have the advantage of a highly ordered three-dimensional structure defined by different and multiple molecular recognition motifs. Proteins can have several binding sites with varying affinities, and the increased complexity of proteins, compared to simple molecular hosts with one binding site, provides a challenge for control of the desired reactivity. HSA and bovine serum albumin (BSA) were used as photochirogenic hosts,[13−16] where a much higher ee was observed for HSA (79% for **2**; 88% for **3** for AC/HSA = 3.0)[13] than for BSA (29% for **2**; 41% for **3** for AC/BSA = 1.3).[16] The reaction between the ACs in the two serum albumins is dynamic,[14,15] and the AC molecules are not located in close proximity in the reactive binding site.[13,16] The same enantiomer of **3*** was formed in excess for both serum albumins while the antipodes were formed in excess for product **2*** in HSA and BSA. The circular dichroism spectral behavior upon titration was different for HSA and BSA at AC/serum albumin ratios of 3 and higher, indicating that the chirality of some of the AC binding environments was different in the two proteins. HSA and BSA have a sequence identity (homology) of 75.6%.[17] HSA and BSA show significant differences in the binding of the same molecules,[18,19] and differences were also observed in the photophysics and photochemistry of bound compounds.[20−23] The reasons for these differences have not been elucidated, since the structure for BSA was only recently reported.[17]

AC photocyclodimerization in a hydrogen-bonded complex with a chiral template showed that the ee is a consequence of the shielding of one of the two prochiral faces of AC.[12] Anisotropy experiments were performed for the HSA/AC system to explore the possibility that the high ee observed was due to the immobilization of AC in the HSA reactive site, since free rotation of AC within the binding site would lead to both prochiral faces of the AC to be accessible for reaction decreasing the ee. The anisotropy studies showed that the immobilization of one of the ACs in HSA is key to achieve the high ee observed.

Theoretical Background. Decays in the emission anisotropy of fluorophores are related to the depolarization of the emission as the fluorophores rotate in solution. Intrinsic protein fluorophores or probes bound to proteins have been used to study the dynamics of proteins.[24] The rotation of proteins is slower than the rotation of small fluorophores in solution. The presence of various populations of fluorophores with different rotational correlation times leads to complex anisotropy decays, as was for example shown for studies with serum albumins.[25−28] Rotational correlation times recovered from the anisotropy decays are related to the difference in intensity of the light with different polarizations. Therefore, the anisotropy and fluorescence decays are collected with similar time windows. The rotational correlation times can be shorter or longer than the fluorescence lifetime of the fluorophore as long as the changes in the intensity difference of the polarized emissions are measurable.

Fluorescence decays (eq 1) are fit to a sum of exponentials defined by the lifetime of each species (τ_i) and its pre-exponential factor (A_i), where the sum of A values is unity. Reconvolution of the instrument response function (IRF) with the calculated fits is required when the IRF width is comparable to the decay, while such a procedure is not required when the excitation pulse is narrow.

$$I(t) = I_0 \sum_{1}^{i} A_i e^{-t/\tau_i} \tag{1}$$

Anisotropy decays are calculated from the fluorescence decays collected at the vertical ($I_{VV}(t)$) and horizontal ($I_{VH}(t)$) positions of the emission polarizer when the samples are excited with vertically polarized light (eq 2).

$$r(t) = \frac{I_{VV}(t) - GI_{VH}(t)}{I_{VV}(t) + 2GI_{VH}(t)} \tag{2}$$

Parameter G corrects for the different sensitivity of the optics to the polarization of light, and the value for G is calculated by exciting the samples with horizontally polarized light and measuring the emission at the vertical ($I_{HV}(t)$) and horizontal ($I_{HH}(t)$) positions of the emission polarizer (eq 3).

$$G = \frac{\int I_{HV}(t)}{\int I_{HH}(t)} \tag{3}$$

Molecules have an intrinsic anisotropy (r_0) that depends on the angle between the absorption and emission transition moments. The value for r_0 depends on the excitation wavelength and can vary between 0.4 for parallel transition moments and −0.2 for orthogonal transition moments.[24] Experimentally, the r_0 value is determined in viscous solutions at low temperature, where the rotation of the molecule is very slow. In time-resolved experiments, all molecules are polarized at the time of excitation, and the initial anisotropy value is expected to be r_0. If the measured value is lower, then a fraction of the molecules underwent rotations that are faster than the time resolution of the experiment.

The number of rotational correlation times observed for a molecule that has one fluorescence lifetime depends on the number of independent rotational axes that lead to a change in the angle between the emission transition moment and the polarizer for the detection optics. A spherical rotor can be assumed when the anisotropy decay is exponential (eq 4) leading to the recovery of one rotational correlation time (ϕ). Equation 4 cannot be used directly when reconvolution of the IRF is required, and the polarized emission intensities ($I_{VV}(t)$, $I_{VH}(t)$) are fit simultaneously.[24,29]

$$r(t) = r_0 e^{-t/\phi} \tag{4}$$

The analysis of the anisotropy decay is more complex for heterogeneous systems with multiple fluorescence lifetimes, since the curvature of the anisotropy decay may not be directly related to the rotation of the individual fluorescent species.[30] The analysis can be carried out using an associated heterogeneous model, which assumes that the fluorescent species have different fluorescence lifetimes and different rotational correlation times. In addition, no interconversion is assumed to occur between the different species during their excited-state lifetimes.[30] The observed anisotropy decay for the sample corresponds to the product of the fractional fluorescence intensity ($f_i(t)$) and the anisotropy ($r_i(t)$) for each species "i" (eq 5). In other words, the contribution to the total anisotropy of the anisotropy of each species at each time point is weighted by the species' fluorescence intensity at that time.[24]

dx.doi.org/10.1021/ja3081555 | J. Am. Chem. Soc. 2013, 135, 203−209

$$r(t) = \sum_{1}^{i} f_i(t) r_i(t) \quad (5)$$

The fractional fluorescence intensities for each species (eq 6) are calculated from the fluorescence lifetimes (τ_i) and the pre-exponential factors (A_i) obtained from the fluorescence decays (eq 1) collected at the magic angle of 54.7°. Detection at the magic angle eliminates any polarization effects on the emission decay.

$$f_i(t) = \frac{A_i e^{-t/\tau_i}}{\sum_1^i A_i e^{-t/\tau_i}} \quad (6)$$

Equation 4 is used to define $r_i(t)$ in eq 5 when each fluorescence lifetime corresponds to a unique fluorescent species in the system that has one rotational correlation time. A more complex scenario occurs when the same fluorescence lifetime corresponds to two or more populations of fluorescent molecules, for example, when the fluorescence lifetime does not change upon incorporation of the fluorophore into different environments. In this case, the anisotropy decay associated to this particular fluorescence lifetime is described by a sum of exponential functions (eq 7), where "j" corresponds to the number of species having the same fluorescence lifetime. Each species has a pre-exponential factor (β_j) and an associated rotational correlation lifetime (ϕ_j). The sum of β_j values is unity.[24]

$$r_i(t) = r_0 \sum_{1}^{j} \beta_j e^{-t/\phi_j} \quad (7)$$

RESULTS

The initial anisotropy of AC measured in a viscous solvent is 0.23 (Supporting Information, Figure S1), and the rotational correlation time for AC in water was estimated to be 0.05 ns (Figure S2, for implementation of the analysis see the Supporting Information). This value was determined on the time scale employed to study the AC/HSA system, and the ϕ value for AC in water could be shorter.

AC binds to four binding sites in HSA, which have decreasing binding affinities with sequential AC binding stoichiometries of 1, 1, 3, and 5.[13] The AC bound to HSA site 1 is unreactive and well protected from quenchers in water, while the AC in site 2 is unreactive and nonfluorescent probably because of efficient quenching by a proximal tryptophan residue.[13,14] Therefore, the ee for **2*** and **3*** is a consequence of AC reactivity in HSA sites 3 and 4. The anisotropy decay for AC at different concentrations of HSA shows that the decay is slowest when AC is bound to site 1 (AC/HSA = 1) and is progressively faster at higher AC/HSA ratios when sites 3 and 4 are populated (Figure 1). The fraction of AC in water appears as a fast offset at time zero, and this fraction is larger at higher AC/HSA ratios.

Analysis of the anisotropy decays requires the determination of experimental conditions where the rotational correlation time for AC in an individual binding site can be recovered. The AC lifetimes (τ) and pre-exponential factors (A) have to be known for the analysis of the anisotropy decay. These parameters were measured with the emission polarizer set at the magic angle. Two lifetimes are observed for AC in site 1 (1.8 and 4.0 ns), while a third lifetime of 15.8 ns is recovered for AC in site 4 and water.[14] These lifetimes were fixed, and the

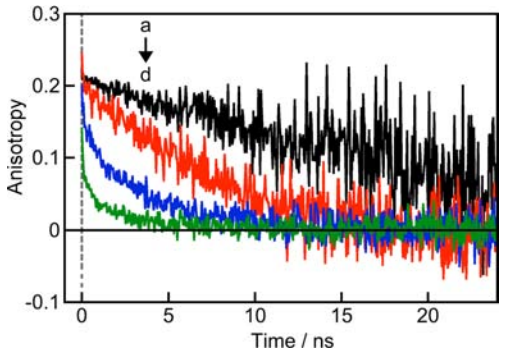

Figure 1. Anisotropy decays for the emission of AC (30 μM) in the presence of HSA. AC/HSA = 1 (a, black); 3 (b, red); 5 (c, blue), and 10 (d, green).

A values were determined (Supporting Information, Table S1). The lifetime for AC in site 3 was previously determined to be between 6 and 9 ns, but this lifetime could only be resolved when inhibitors were used that displace AC from site 1 so that the fraction of AC in site 3 was increased.[14] Diflunisal (DIF) was used as an inhibitor. DIF is known to bind to HSA Sudlow drug site II (subdomain IIIA),[31,32] which is the site that was previously assigned to AC binding site 1.[14] DIF was also shown to bind to a secondary site at the interface of subdomains IIA and IIB and to bind more weakly to the Sudlow drug binding site I,[31] which was previously assigned to AC bound to HSA site 2.[14] AC was excited at 375 nm, and DIF does not emit when excited at this wavelength (Supporting Information, Figures S3 and S4). Circular dichroism spectral titration experiments showed that, in the presence of an equimolar amount of DIF, AC does not bind to site 1 (Figure 2). At

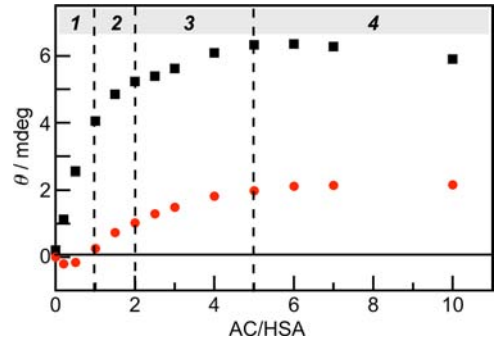

Figure 2. Changes in the induced circular dichroism signal (ellipticity, θ) for AC at 389 nm when AC (0–300 μM) was added to HSA (30 μM) in the presence (red circles) or absence (black squares) of 150 μM DIF added as an inhibitor. The dotted lines and the numbers at the top of the figure indicate the different HSA binding sites for AC.

higher AC/HSA ratios when AC binds to sites 2 and 3, the increments for θ are similar in the absence and presence of DIF, indicating that AC binding to sites 2 and 3 was not inhibited. However, a difference was observed for θ for AC/HSA ratios above 5, where a decrease was observed for θ in the absence of DIF, but the θ value is constant in the presence of the inhibitor, suggesting that DIF was able to bind to HSA site 4. This result suggests that the AC in site 4 of HSA corresponds to the secondary binding site for DIF assigned to the site at the interface of subdomains IIA and IIB. Binding of DIF to HSA site 2 is probably too weak to compete. The binding of DIF to

dx.doi.org/10.1021/ja3081555 | J. Am. Chem. Soc. 2013, 135, 203–209

sites 1 and 4 of HSA was instrumental in determining the rotational correlation time for AC in site 3 (see below).

The anisotropy decay (for implementation of the analysis see the Supporting Information) of the singlet excited state of AC bound to HSA site 1 (AC/HSA = 0.2) showed a predominant component with a rotational correlation time of 55 ± 5 ns and a r_0 value of 0.21 ± 0.01 (Supporting Information, Figure S5). Only a minor amount of AC underwent fast depolarization because the measured r_0 value is close to the one determined in a homogeneous solvent (0.23). The ϕ value of 55 ns for AC in site 1 is within the range previously determined for the rotation of HSA or BSA (39−53 ns)[33−38] and shows that AC in site 1 of HSA is immobile and does rotate with the protein. The minor (A_3 < 0.01) AC species with a fast anisotropy decay is likely due to heterogeneity in HSA (see the Supporting Information for details).

Excited AC in HSA site 1 has two lifetimes, which were assigned to the binding of AC in two different orientations within this site.[14,15] A fast exchange between these two orientations would have led to a depolarization of the emission and is unlikely given the long ϕ and high r_0 values measured. Simulations were performed by fixing one of the ϕ values to 55 ns and varying the second one (Supporting Information, Figures S6 and S7), which showed that a deviation of the fit from the experimental data would have been observed if one of the rotational correlation times was shorter than 30 ns. The simulations and the high r_0 value suggest that both orientations of AC in site 1 are immobile and nonexchangeable.

The rotational correlation time for AC bound to site 3 was determined from measurements in the presence of the inhibitor DIF. Four lifetimes were recovered for the emission of AC bound to HSA in the presence of DIF (Supporting Information, Tables S2 and S3). The four lifetimes in the presence of 10 equivalents of DIF and an AC/HSA ratio of 1 were assigned to AC in site 1 (1.8 and 4.0 ns), site 3 (8.2 ns), and water (15.8 ns). The anisotropy decay shows fast and slow components (Figure 3). The data were analyzed using the

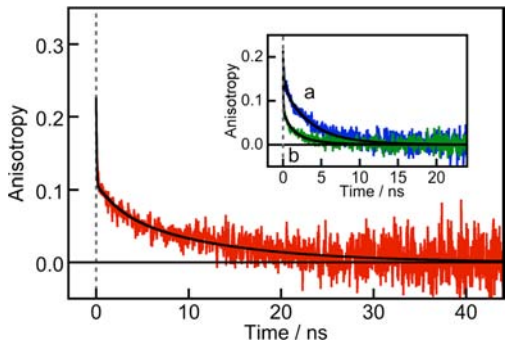

Figure 3. Anisotropy decays for the emission of AC (30 μM) in the presence of HSA (30 μM) and the inhibitor DIF (300 μM). The solid line corresponds to the fit of the data to eqs 5 and 6. The inset shows the fit (black lines) of the anisotropy decays for the emission of AC (30 μM) in the presence of 6 μM (a, blue) and 3 μM (b, green) HSA to eqs 5−7.

associated heterogeneous model (eqs 5 and 6), where the fractional intensities were calculated from the pre-exponential and lifetime values recovered from the fluorescence decay measured at the magic angle. The rotational correlation times for AC in site 1 (55 ns) and in water (0.05 ns) were fixed for the fit of the anisotropy decay. The recovered rotational correlation time for AC in site 3 was determined to be 36 ± 5 ns (for residuals see the Supporting Information, Figure S8) while the r_0 value for the fit was 0.23 ± 0.01 (Supporting Information, Table S4). The anisotropy decay in the presence of 5 equivalents of DIF could be fit by fixing the lifetime and rotational correlation time for AC in site 3 (Supporting Information, Figure S9), showing that these results are consistent with the rotational correlation time determined at the higher concentration of DIF. Fits of the anisotropy decay in the presence of 10 equivalents of DIF where the rotational correlation time for AC in site 3 was fixed to values lower than 30 ns led to inadequate fits while the fits were adequate for a ϕ value of 50 ns for AC in site 3 (Supporting Information, Figure S10), showing that the fit to the anisotropy decay is not very sensitive to the upper value of ϕ.

The rotational correlation time for AC in site 4 of HSA was measured in the absence of DIF, because this inhibitor displaces AC from site 4. However, the longest lifetime measured (15.8 ns, Table S1 of the Supporting Information) corresponds to AC in site 4 and in water.[14] For this reason, the anisotropy decay was fit assuming three lifetimes (inset Figure 3; for residuals see the Supporting Information, Figure S8) but with two rotational correlation times for the species with 15.8 ns (eqs 5,6 (i = 3), and 7 (j = 2)). One rotational correlation time for the 15.8 ns component was fixed to 0.05 ns for AC in water, and a rotational correlation time of approximately 0.7−0.8 ns was recovered for AC in site 4 of HSA (Supporting Information, Table S4). It is important to note that this rotational correlation time has a large error and it should be seen as an estimate. Nevertheless, ϕ for AC in site 4 is slower than that for AC in water but faster than that for AC in sites 1 or 3, showing that AC in site 4 is only partially immobilized, probably on the protein exterior.

The effect of DIF on the photocyclodimerization of AC (Table 1) is indicative of the displacement of AC from the unreactive site 1 of HSA leading to a progressive increase in the photoconversion as the concentration of DIF was raised. Addition of DIF enhanced the HT/HH ratio suggesting that the relative population of sites 3 and 4 was changed, which is in line with the displacement by DIF of AC from site 4. The ee for **2*** and **3*** increased up to 5 equivalents of DIF and decreased at higher DIF concentrations. This result suggests that, at the high DIF concentration, some of the reactions were occurring for AC in water, while at the lower DIF concentrations, the contribution from the reaction in water is negligible.

DISCUSSION

Mechanistic studies for the AC−HSA system are complex because of the multiple binding sites in the protein. In addition, the usual techniques used to obtain structural information, for example, X-ray crystallography or NMR spectroscopy, are not amenable for small molecules bound to sites with moderate to weak binding affinities. The combination of the use of an inhibitor, which binds to the unproductive site 1 and also to site 4, made it possible to analyze the anisotropy decay for AC bound to site 3.

The rotational correlation time for AC in site 3 is 36 ns, while it is approximately 0.7−0.8 ns in site 4. A high ee is observed for the reaction in site 3 whereas the ee is moderate in site 4,[13,14] showing that the immobilization of AC is essential to achieve a high ee. The ee of 80−90% in site 3 suggests that one of the prochiral *re*/*si*-faces of AC is covered leaving the other face exposed to react with the second AC molecule. The high

dx.doi.org/10.1021/ja3081555 | J. Am. Chem. Soc. 2013, 135, 203−209

Table 1. HSA-Mediated Photocyclodimerization of AC (30 μM) in the Presence and Absence of DIF as an Inhibitor[a]

			product distribution/%				ee[b]/%		
HSA/μM	DIF/μM	conversion/%	**1**	**2***	**3***	**4**	**2***	**3***	HT/HH[c]
0	0	91	37	35	17	11	0	0	2.6 ± 0.3
30	0	15	36	41	15	8	71	85	3.3 ± 0.5
	30	16	36	43	13	8	80	89	3.8 ± 0.6
	60	33	36	41	15	8	84	93	3.3 ± 0.5
	150	40	41	43	10	6	86	92	5 ± 1
	300	48	48	40	7	5	76	71	7 ± 2

[a]Irradiated at >320 nm for 1 h under N_2 in phosphate buffer (pH 7.0) at room temperature. Errors for the product distribution are ±2%, the error for the ee of **2*** is ±2%, and for the ee of **3***, the error is 5%. [b]Enantiomeric excess determined by chiral HPLC analysis using a tandem ODS + OJ-RH column. [c](**1** + **2***)/(**3*** + **4**)

ee suggests that the three AC molecules in site 3 have the same prochiral face protected. The absolute configurations of the AC dimers were recently determined,[39,40] and the positive ee for **2*** and **3*** in HSA indicates that the *si*−*si* products are formed for **2*** and **3***. However, the formation of the *si*−*re* products also occurs, since products **1** and **4** were formed. This result suggests that one of the ACs involved in the bimolecular reaction is released from the protein wall. The released AC can rotate leading to the formation of both types of encounter complexes (Scheme 2). It is crucial that the original *re*/*si*-face

Scheme 2. Cartoon Representation of the Reaction of AC in Site 3 of HSA[a]

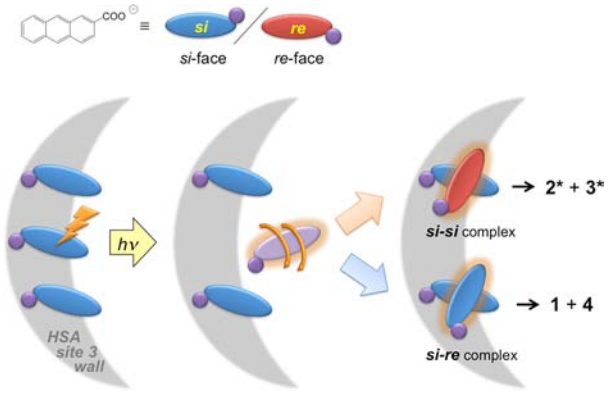

[a]The *si*-face of AC is shown in blue, the *re*-face is shown in red, and the HSA "wall" is shown in grey. Panel (a) shows all three ACs bound to HSA's site 3, exposing the *si*-face; (b) shows the "release" and subsequent "tumbling" of one AC; and (c) shows the two possible encounter complexes (*si*−*si* and *si*−*re*) leading to cyclodimer pairs, **2*** + **3*** and **1** + **4**, respectively. The blue and red colors in this scheme always indicate the *si*- and *re*-faces that are exposed to the viewer. Hence, the *si*−*si* complex, in which the *si*-faces of two ACs are facing each other, exposes the *si*-face of the AC molecule on the back and the *re*-face of the AC in the front.

selectivity upon adsorption to the protein wall exclusively determines the absolute configurations and the ee's of chiral cyclodimers **2*** and **3***, while the rotation of one AC never deteriorates the products' ee but simply leads to the formation of cyclodimers **1** and **4**, respectively. The detachment from the wall leads to the loss of chirality memory for the released AC, but the enantioselectivity is fully secured and transferred to the chiral cyclodimers by the AC held on the wall. However, the free rotation of the detached AC leads to the scrambling of the cyclodimers produced. The product distributions observed for the HSA-mediated photocyclodimerization are similar to that observed for free AC. This may indicate that the void space of site 3 is relatively large and/or the released AC has to travel a relatively long distance (enough to lose the original orientational information) before meeting the AC immobilized in the same site. This mechanism is in nice agreement with the lack of exciton coupling in the circular dichroism spectrum. It is likely that AC is released from the protein wall upon excitation, because of its lower acidity (pK_a^* = 6.6) when compared to the AC ground state (pK_a = 4.2).[41] The binding sites inside HSA are somewhat isolated from bulk water and are likely more hydrophobic. Therefore, the pH of the aqueous solution does not immediately translate into a pH inside the binding site. In this site, with increased hydrophobicity, the reduced acidity of AC will weaken the interaction with cationic amino acid residues such as lysine and arginine, which may be involved in the interaction of AC with the wall of HSA. The shorter rotational correlation time for AC in site 3 than observed for AC in site 1 could indicate an average value that includes a small portion of the "released" AC that can rotate. Reaction of an AC in site 3 with a ground-state AC in water is unlikely considering the low concentrations of free AC at the AC, HSA, and DIF concentrations used. An orthogonal encounter complex was previously suggested for the photocyclodimerization of AC using a hydrogen-bonding template, based on the value close to unity for the (**2*** + **3***)/(**1** + **4**) ratio.[12] This ratio is somewhat higher for the reaction in HSA (1.3 ± 0.1) suggesting that some preference exists for the relative orientation of the carboxylate moieties in the encounter complex. As expected, the ratio decreases once AC is located in site 4 and water, that is, when the DIF concentration was increased to 5 and 10 equivalents, where the ACs are more mobile.

In summary, this study uncovered that the key to achieve a high ee for a bimolecular reaction using the supramolecular approach is that one of the two reactants is immobilized so that only one of the prochiral faces is exposed and can undergo reaction. The presence of a confined environment with more than one reactant is also required. This confined space ensures that no reaction occurs in nonchiral environments such as the homogeneous phase. The high ee for the reaction in HSA when compared to the reaction in BSA is due to the immobilization of all ACs with the same exposed prochiral face in the case of HSA. This is not the case for BSA as indicated by the different signs for the induced circular dichroism signals when the AC is bound to these two proteins.[13] Therefore, the final requirement to achieve a high ee is that all reactants in the confined space should have the same prochiral face protected by the supramolecular host. From the dynamic point of view, the release of one of the reactants from the protein wall as well as

dx.doi.org/10.1021/ja3081555 | J. Am. Chem. Soc. 2013, 135, 203−209

the slow mobility in the site are essential to secure the high prochiral face selectivity achieved upon attachment of the reactants to the wall of the protein.

EXPERIMENTAL SECTION

Human serum albumin (HSA, Sigma–Aldrich, fat-free grade, lot 109K7550 with purity of >99% with 0.004% of fatty acids), 2-anthracenecarboxylic acid (AC, Tokyo Chemical Industry), diflunisal (DIF, Sigma–Aldrich), standardized sodium hydroxide solution (Anachemia, ACS reagent grade), sodium hydrogen phosphate (99%, Anachemia), potassium dihydrogen phosphate (99%, BDH), and propylene glycol (>99.5%, Sigma–Aldrich) were used as received. AC and DIF showed monoexponential fluorescence decays indicating the absence of any fluorescent impurities. Deionized water from a Barnstead Nanopure system was used to prepare the solutions (≥17.8 MΩ cm^{-1}).

AC stock solutions (1 mM) were prepared in 10 mM aqueous NaOH. Phosphate buffer pH 7.0 (33 mM) was prepared by mixing Na_2HPO_4 and KH_2PO_4 aqueous solutions in a ratio of 2:1. DIF (2.5 mM) and HSA (0.1 mM and 0.5 mM) stock solutions were prepared in buffer. Solutions containing AC, HSA, and DIF were prepared by diluting the appropriate amount of stock solutions in buffer. All experiments were performed at 25 °C, and previous reports using circular dichroism experiments suggest that conformational changes occur only at temperatures higher than 50 °C.[13,42] The concentration of AC was kept constant at 30 μM, while the concentration of HSA was varied between 3 and 150 μM to achieve different AC/HSA concentration ratios.

Product studies were carried out at room temperature. A 3 mL aliquot of the solution was deaerated using three freeze–pump–thaw cycles and was kept under N_2. The solution was irradiated for 1 h at wavelengths longer than 320 nm using a high-pressure mercury lamp (300 W) fit with a uranium glass filter. A 400 μL aliquot of the irradiated solution was added to an equivalent amount of acetonitrile and was left to stand overnight. The resultant solution was filtered through ultrafiltration and used for the high-performance liquid chromatography (HPLC) analysis on a Shimadzu Prominence instrument equipped with a fluorescence detector (excitation at 254 nm and observation at 420 nm)[43] and a tandem column of Cosmosil 5C18-AR-II (Nakarai) and Chiralcel OJ-RH (Daicel) at 35 °C eluted with a 36:64 mixture of acetonitrile and water containing 0.1% trifluoroacetic acid.[12,43]

Absorption spectra were measured on a Varian Cary 1 spectrophotometer at room temperature. Fluorescence emission spectra were measured with a PTI-QM2 fluorimeter at 25.0 ± 0.1 °C using 1 nm bandwidths for the excitation and emission monochromators. Circular dichroism spectra were measured on a JASCO J-720WI with a temperature controller (PMH-354WI). Time-resolved anisotropy measurements were collected on an Edinburgh Instruments OB920 single photon counting system at 25.0 ± 0.1 °C. The samples were excited with vertically polarized light from a 378 nm laser diode (EPL-375, Edinburgh Instruments, full width at half-maximum (FWHM) of 6 nm), and the intensity of the incident light was controlled with a neutral density filter. The emission was collected at 440 nm using a time-window of 50 ns and a 90° degree geometry between the excitation and detection optics. The repetition rate of the laser pulses was 2 MHz, and the stop-rate was 0.1% of the start-rate. The emission was collected through a polarizer (Glan–Thompson prism, Edinburgh Instruments) mounted in front of a monochromator (16 nm bandwidth). The decays were collected for the same amount of time with the polarizers set either at the vertical or the horizontal positions. The intensity was about 10 000 counts in the channel of maximum intensity for the decay collected with the polarizer set at the vertical position. The detector was a microchannel plate photomultiplier (Hamamatsu R3809U-50), and the detection system from Edinburgh Instruments had a time resolution of approximately 25 ps. Fluorescence decays for the determination of lifetimes and their pre-exponential factors were collected with the emission polarizer set at the magic angle (54.7°) in order to eliminate any polarization effects due to the use of a polarized laser excitation source. The IRF was determined by detecting the scattered light at 378 nm with a dilute Ludox solution. The shortest total collection time employed was 50 ns. On this time scale, the IRF was narrow, and the FWHM was defined by 3 time-channels out of 1024.

Anisotropy measurements in propylene glycol as a viscous solvent were performed at −50 °C using a cryostat to control the temperature (USP-203, Unisoku) and a photomultiplier as the detector (Hamamatsu R1527), which has a time resolution of 0.5 ns.

ASSOCIATED CONTENT

Supporting Information

AC initial anisotropy; lifetime analysis for AC and AC/HSA in the presence and absence of DIF; anisotropy decay for AC in water; absorption and fluorescence spectra for DIF; anisotropy decays of AC in HSA sites 1, 3, and 4, AC. This material is available free of charge via the Internet at http://pubs.acs.org.

AUTHOR INFORMATION

Corresponding Author

cornelia.bohne@gmail.com; inoue@chem.eng.osaka-u.ac.jp

Present Address

[‖]Laboratorio de Química Biológica, Facultad de Química, Pontificia Universidad Católica de Chile, Santiago, Chile.

Notes

The authors declare no competing financial interest.

ACKNOWLEDGMENTS

This work was supported by the Natural Sciences and Engineering Research Council of Canada (NSERC), Japan Society for the Promotion of Science (Grant-in-Aid for Scientific Research nos. 24655029, 23750129, 23350018, and 21245011), Mitsubishi Chemical Corporation Fund, Sumitomo Foundation, Shorai Foundation for Science and Technology, and Kurata Memorial Hitachi Science and Technology Foundation.

REFERENCES

(1) van Leeuwen, P. W. N. M. *Supramolecular Catalysis*; Wiley-VCH: Weinheim, Germany, 2008.

(2) Wada, T.; Inoue, Y. In *Chiral Photochemistry*; Inoue, Y., Ramamurthy, V., Eds.; Marcel Dekker: New York, 2004; pp 341–384.

(3) Yang, C.; Inoue, Y. In *Supramolecular Photochemistry: Controlling Photochemical Processes*; Ramamurthy, V., Inoue, Y., Eds.; John Wiley & Sons: Singapore, 2011; pp 115–153.

(4) Bauer, A.; Westkämper, F.; Grimme, S.; Bach, T. *Nature* **2005**, *436*, 1139–1140.

(5) Ke, C.; Yang, C.; Mori, T.; Wada, T.; Liu, Y.; Inoue, Y. *Angew. Chem., Int. Ed.* **2009**, *48*, 6675–6677.

(6) Wang, Q.; Yang, C.; Ke, C.; Fukuhara, G.; Mori, T.; Liu, Y.; Inoue, Y. *Chem. Commun.* **2011**, *47*, 6849–6851.

(7) Nakamura, A.; Inoue, Y. *J. Am. Chem. Soc.* **2003**, *125*, 966–972.

(8) Nakamura, A.; Inoue, Y. *J. Am. Chem. Soc.* **2005**, *127*, 5338–5339.

(9) Yang, C.; Mori, T.; Origane, Y.; Ko, Y. H.; Selvapalam, N.; Kim, K.; Inoue, Y. *J. Am. Chem. Soc.* **2008**, *130*, 8574–8575.

(10) Bach, T.; Bergmann, H.; Grosch, B.; Harms, K. *J. Am. Chem. Soc.* **2002**, *124*, 7982–7990.

(11) Müller, C.; Bauer, A.; Maturi, M. M.; Cuquerella, M. C.; Miranda, M. A.; Bach, T. *J. Am. Chem. Soc.* **2011**, *133*, 16689–16697.

(12) Kawanami, Y.; Pace, T. C. S.; Mizoguchi, J.-I.; Yanagi, T.; Nishijima, M.; Mori, T.; Wada, T.; Bohne, C.; Inoue, Y. *J. Org. Chem.* **2009**, *74*, 7908–7921.

(13) Nishijima, M.; Wada, T.; Mori, T.; Pace, T. C. S.; Bohne, C.; Inoue, Y. *J. Am. Chem. Soc.* **2007**, *129*, 3478–3479.

(14) Pace, T. C. S.; Nishijima, M.; Wada, T.; Inoue, Y.; Bohne, C. *J. Phys. Chem. B* **2009**, *113*, 10445−10453.
(15) Nishijima, M.; Pace, T. C. S.; Nakamura, A.; Mori, T.; Wada, T.; Bohne, C.; Inoue, Y. *J. Org. Chem.* **2007**, *72*, 2707−2715.
(16) Wada, T.; Nishijima, M.; Fujisawa, T.; Sugahara, N.; Mori, T.; Nakamura, A.; Inoue, Y. *J. Am. Chem. Soc.* **2003**, *125*, 7492−7493.
(17) Majorek, K. A.; Porebski, P. J.; Dayal, A.; Zimmerman, M.; Jablonska, K.; Stewart, A. J.; Chruszcz, M.; Minor, W. *Mol. Immunol.* **2012**, *52*, 174−182.
(18) Kragh-Hansen, U. *Pharmacol. Rev.* **1981**, *33*, 17−53.
(19) Peters, Jr., T. *All about Albumin: Biochemistry, Genetics, and Medical Applications*; Academic Press: San Diego, CA, 1996.
(20) Mi, Z.; Burke, T. G. *Biochemistry* **1994**, *33*, 12540−12545.
(21) Ouchi, A.; Zandomeneghi, G.; Zandomeneghi, M. *Chirality* **2002**, *14*, 1−11.
(22) Pérez-Ruiz, R.; Alonso, R.; Nuin, E.; Andreu, I.; Jiménez, M. C.; Miranda, M. A. *J. Phys. Chem. B* **2011**, *115*, 4460−4468.
(23) Vayá, I.; Jiménez, M. C.; Miranda, M. A. *J. Phys. Chem. B* **2008**, *112*, 2694−2699.
(24) Lakowicz, J. R. *Principles of Fluorescence Spectroscopy*, 4th ed.; Springer: New York, 2006.
(25) Bhattacharya, B.; Nakka, S.; Guruprasad, L.; Samanta, A. *J. Phys. Chem. B* **2009**, *113*, 2143−2150.
(26) Dobretsov, D. G.; Syreishchikova, T. I.; Gryzunov, Y. A.; Smolina, N. V.; Komar, A. A. *Biophysics* **2010**, *55*, 182−187.
(27) Sahu, K.; Mondal, S. K.; Ghosh, S.; Roy, D.; Bhattacharyya, K. *J. Chem. Phys.* **2006**, *124*, 124909.
(28) Sinha, S. S.; Mitra, R. K.; Pal, S. K. *J. Phys. Chem. B* **2008**, *112*, 4884−4891.
(29) Cross, A. J.; Fleming, G. R. *Biophys. J.* **1984**, *46*, 45−56.
(30) Ludescher, R. D.; Peting, L.; Hudson, S.; Hudson, B. *Biophys. Chem.* **1987**, *28*, 59−75.
(31) Ghuman, J.; Zunzzain, P. A.; Petitpas, I.; Bhattacharya, A. A.; Otagiri, M.; Curry, S. *J. Mol. Biol.* **2005**, *353*, 38−52.
(32) Mao, H.; Hajduk, P. J.; Craig, R.; Bell, R.; Borre, T.; Fesik, S. W. *J. Am. Chem. Soc.* **2001**, *123*, 10429−10435.
(33) Castellano, F. N.; Dattelbaum, J. D.; Lakowicz, J. R. *Anal. Biochem.* **1998**, *255*, 165−170.
(34) Ferrer, M. L.; Duchowicz, R.; Carrasco, B.; García de la Torre, J.; Acuña, A. U. *Biophys. J.* **2001**, *80*, 2422−2430.
(35) Helms, M. K.; Petersen, C. E.; Bhagavan, N. V.; Jameson, D. M. *FEBS Lett.* **1997**, *408*, 67−70.
(36) Lakowicz, J. R.; Gryczynski, I. *Biophys. Chem.* **1992**, *45*, 1−6.
(37) Sardar, P. S.; Samanta, S.; Maity, S. S.; Dasgupta, S.; Ghosh, S. *J. Phys. Chem. B* **2008**, *112*, 3451−3461.
(38) Terpetschnig, E.; Szmacinski, H.; Malak, H.; Lakowicz, J. R. *Biophys. J.* **1995**, *68*, 342−350.
(39) Wakai, A.; Fukusawa, H.; Yang, C.; Mori, T.; Inoue, Y. *J. Am. Chem. Soc.* **2012**, *134*, 4990−4997.
(40) Wakai, A.; Fukusawa, H.; Yang, C.; Mori, T.; Inoue, Y. *J. Am. Chem. Soc.* **2012**, *134*, 10306−10306.
(41) Donckt, E. V.; Porter, G. *Trans. Faraday Soc.* **1968**, *64*, 3215−3217.
(42) Shaw, A. K.; Pal, S. K. *J. Photochem. Photobiol., B* **2008**, *90*, 69−77.
(43) Nishijima, N.; Wada, T.; Nagamori, K.; Inoue, Y. *Chem. Lett.* **2009**, *38*, 726−727.